Dalton Transactions

Accepted Manuscript

ROYAL SOCIETY OF CHEMISTRY

www.rsc.org/dalton

Tetracyanobutadiene functionalized ferrocenyl BODIPY dyes

Bhausaheb Dhokale, Thaksen Jadhav, Shaikh M. Mobin, and Rajneesh Misra[*]

Department of Chemistry, Indian Institute of Technology Indore 452 017 (India)

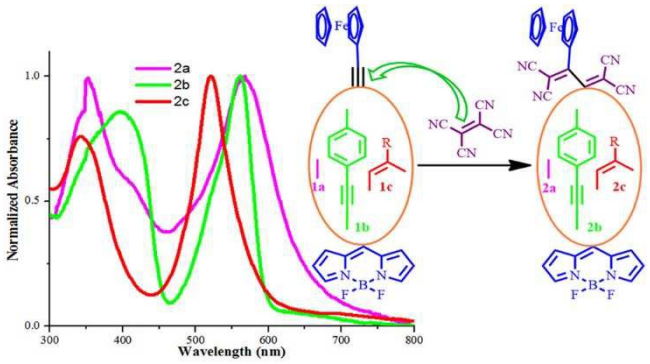

Abstract

The tetracyanobutadiene (TCBD) derivatives of ferrocenyl BODIPYs **2a – 2c** were designed and synthesized by [2+2] cycloaddition-retroelectrocyclization reaction of tetracyanoethylene (TCNE) with *meso* alkynylated ferrocenyl BODIPYs. The TCBD substituted ferrocenyl BODIPYs were designed in such a way, that the distance between the ferrocenyl unit and the TCBD remains constant, whereas the distance between the BODIPY and the TCBD unit varies. The TCBD and BODIPY units were connected directly through single bond (in **2a**), through phenylacetylene linkage (in **2b**) and through vinyl linkage (in **2c**). The photonic and electrochemical properties of ferrocenyl BODIPYs were strongly perturbed by the incorporation of TCBD. The TCBD derivatives **2a – 2c** show red shifted absorption compared to their precursors **1a – 1c**. The single crystal structures of TCBD functionalized ferrocenyl BODIPYs **2a** and **2c** reveal extensive intermolecular hydrogen bonding but lacks the π-π stacking interactions.

Introduction

The donor-acceptor (D-A) systems have gained considerable attention of the scientific community due to their applications in optoelectronic devices.[1] The BODIPY (4,4-Difluoro-4-bora-3a,4a-diaza-*s*-indacene) dyes are known for their unique properties like strong absorption

and emission with high quantum yield, high thermal and photochemical stability and ease of synthetic functionalization.[2] The ferrocenyl derivatives exhibit strong NLO response, rich electrochemistry and high thermal and photochemical stability.[3] Our group and others have explored the ferrocenyl BODIPYs for non-linear optics and multiphoton absorbing materials.[4]

The BODIPY is a strong acceptor, and its electron accepting strength and photonic properties can be tuned by incorporation of suitable functionality at appropriate position.[5] Diederich *et al.* have developed the strong acceptor tetracyanobutadiene (TCBD) by the reaction of tetracyanoethylene (TCNE) with various alkynes.[6] The incorporation of TCBD in the ferrocenyl BODIPY will results stronger D-A system, which is expected to perturb its photonic properties.[7] The incorporation of donor at the *meso* position of the BODIPY leads to blue shift in the absorption, whereas incorporation of acceptor leads to red shift.[8]

We were interested to evaluate the reactivity of ferrocenyl BODIPYs (**1a – 1c**) towards tetracyanoethylene (TCNE) and the effect of TCBD acceptor on the photonic and electrochemical properties of BODIPYs **2a – 2c**. The TCBD substituted ferrocenyl BODIPYs were designed and synthesized in such a way that the distance between ferrocenyl unit and TCBD remains constant, whereas the distance between the BODIPY and the TCBD unit varies. The TCBD and BODIPY were connected directly, through phenylacetylene linkage and vinyl linkage.

Results and discussion

The *meso* TCBD substituted ferrocenyl BODIPYs **2a – 2c** were designed and synthesized by the [2+2] cycloaddition-retroelectrocyclization reaction of ferrocenyl alkyne substituted BODIPYs (**1a – 1c**) with TCNE (Scheme 1). The ferrocenyl alkyne substituted BODIPY **1a** and **1b** were synthesized by the Sonogashira cross-coupling reaction of 8-chloro BODIPY with respective ferrocenyl alkynes.[9] The ferrocenyl enyne substituted BODIPY **1c** was synthesized by the Pd-Cu catalyzed hydroalkynylation reaction of 8-(biphenylethynyl)-BODIPY with ethynylferrocene.[10] The BODIPY **1a** undergoes [2+2] cycloaddition-retroelectrocyclization reaction with TCNE at 40 °C within 8 hours in CH_2Cl_2 solvent and resulted in BODIPY **2a**. The BODIPY **1b** undergoes similar transformation to BODIPY **2b** at room temperature, in 2 hours in CH_2Cl_2 solvent, whereas the BODIPY **1c** took 8 days at 40 °C in CH_2Cl_2 solvent to complete similar reaction and resulted BODIPY **2c**.

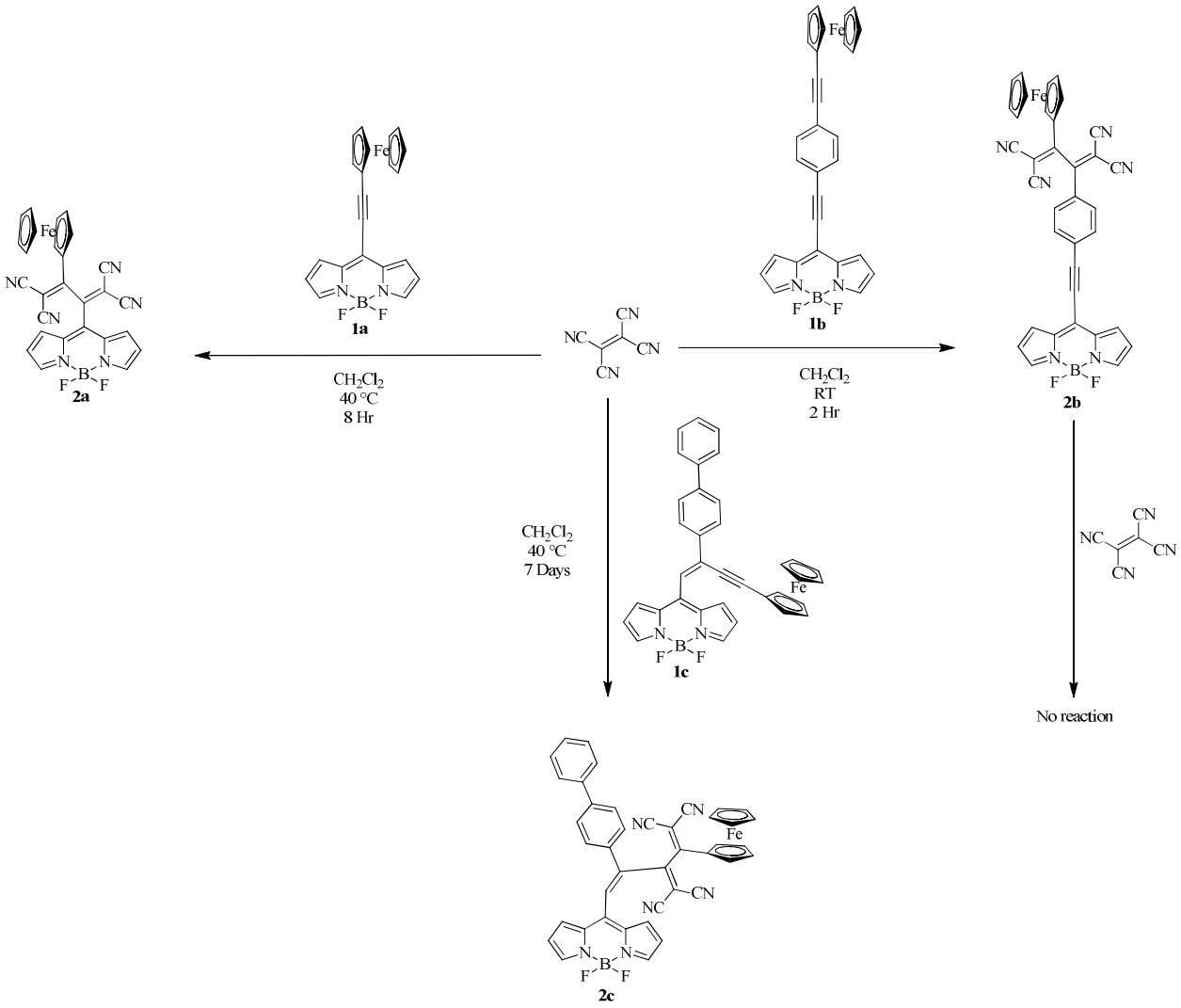

Scheme 1. Synthesis of BODIPYs **2a – 2c**.

The reactivity of the BODIPYs **1a – 1c** towards [2+2] cycloaddition-retroelectrocyclization reaction follows the order **1b**>**1a**>**1c**. The reactivity of alkyne bond towards TCNE was favored by electron rich substituents and disfavored by electron deficient substituents and steric crowding.[11] In BODIPYs **1a – 1c**, the strong electron donor ferrocene and alkyne unit are constant, therefore their reactivity was influenced by the linking bridge between alkyne unit and the BODIPY moiety. The high reactivity of BODIPY **1b** is attributed to the longer distance between the alkyne unit and the electron deficient BODIPY, which resists the delocalization of electron density from alkyne unit to the BODIPY, making the alkyne unit relatively electron rich and reactive. In BODIPY **1a** the alkyne bond is at the *meso* position of electron withdrawing BODIPY moiety, which makes it electron deficient and poorly reactive. In

case of BODIPY **1c** the steric crowding resists the space demand for accommodating the TCBD unit.

The alkyne unit at the *meso* position of the BODIPY undergoes [2+2] cycloaddition-retroelectrocyclization reaction in BODIPY **1a**, but fails to undergo similar reaction in BODIPY **2b**. In BODIPY **1a** the ferrocenyl group maintains the electron density at the alkyne unit against the electron withdrawing BODIPY moiety, whereas in BODIPY **2b** both the BODIPY and TCBD withdraw the electron density from alkyne unit making it electron deficient and inert towards the [2+2] cycloaddition-retroelectrocyclization reaction.[12]

The BODIPYs **2a – 2c** were well characterized by NMR and HRMS techniques. The TCBD substituted BODIPYs **2a** and **2c** were also characterized by single crystal X-ray crystallography.

Photophysical Properties

The electronic absorption spectra of the BODIPYs **1a – 1c** and **2a – 2c** were recorded in toluene (Figure 1) and the corresponding data are shown in Table 1. The BODIPYs exhibit $S_0 \rightarrow S_1$ absorption band at 500 – 570 nm region, and $S_0 \rightarrow S_2$ absorption band at 360 – 400 nm region. The $S_0 \rightarrow S_1$ absorption band of BODIPYs **1a – 1c** show successive red shift with increasing conjugation and follows the order **1b>1a>1c**. In BODIPY **1c**, the *meso* substituent and the BODIPY core adopts non-planar orientation, which breaks the conjugation leading to the blue shifted absorption.

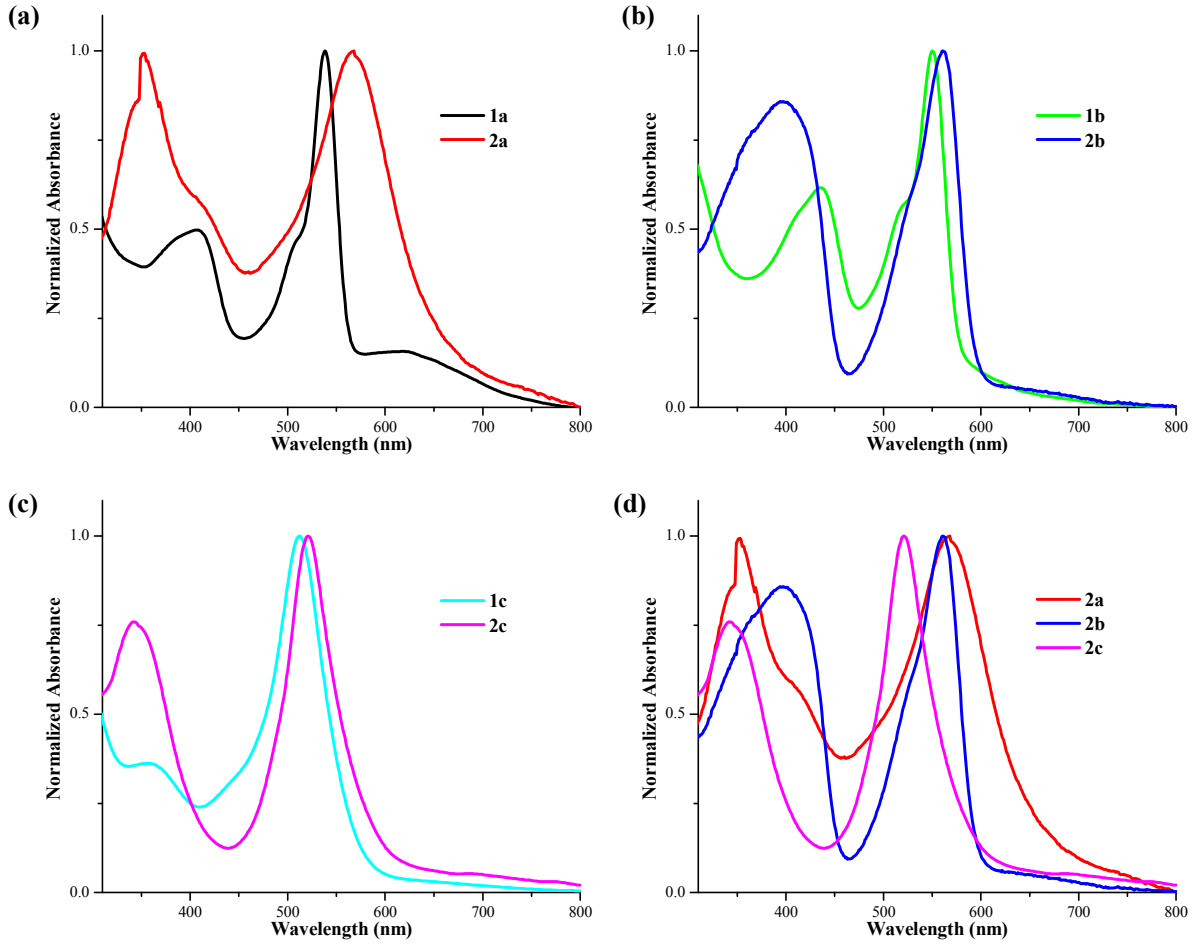

Figure 1. Comparison of normalized electronic absorption spectra of (a) BODIPYs **1a** and **2a**; (b) BODIPYs **1b** and **2b**; (c) BODIPYs **1c** and **2c** and (d) BODIPYs **2a** – **2c**.

The introduction of TCBD unit strongly perturbs the photonic properties of the BODIPYs **2a** – **2c**. The TCBD derivatives **2a**, **2b** and **2c** show 29 nm, 11 nm and 9 nm red shifted absorption compared to BODIPYs **1a**, **1b** and **1c** respectively. This indicates that, even though the TCBD acceptor at the *meso* position disturbs the conjugation it induces the red shift in $S_0 \rightarrow S_1$ absorption band. This is in contrast with the previously reported TCBD derivatives of BODIPY, where the incorporation of TCBD at the *β*-position resulted blue shift in the absorption.[13] The red shift in the absorption band due to the acceptor at *meso* position which is attributed to the efficient stabilization of LUMO than HOMO (Figure 3; Computational calculations).

The absorption band in 360 – 400 nm region corresponds to the $S_0 \rightarrow S_2$ transition. The $S_0 \rightarrow S_2$ absorption band in **2a – 2c** show blue shift with increased intensity on incorporation of TCBD than their precursors **1a – 1c**. The band at 616 nm in BODIPY **1a** is attributed to the charge transfer from donor ferrocene to the acceptor BODIPY. This charge transfer band was not observed in BODIPY **2a**, as it might have been merged in the $S_0 \rightarrow S_1$ absorption band as evidenced from the broadening of the band. The TCBD substituted ferrocenyl BODIPYs are non-emissive in nature.

Table 1. Photophysical properties of BODIPYs **1a – 1c** and **2a – 2c.**[a]

BODIPY	λ_{max} (nm)	$\varepsilon/10^4$ ($M^{-1}.cm^{-1}$) [a]	HOMO-LUMO gap (eV) (Theoretical)[b]
1a	538	4.4	2.86
2a	567	3.4	2.22
1b	550	4.7	2.60
2b	561	4.9	2.31
1c	512	4.6	2.56
2c	521	4.5	1.84

[a]Recorded at λ_{max} in toluene, [b]From DFT calculation.

Electrochemical Properties

The electrochemical analysis of BODIPYs **1a – 1c** and **2a – 2c** were performed in CH_2Cl_2 solvent using 0.1 M tetrabutylammonium hexafluorophosphate as supporting electrolyte (Figure 2 and Figure S6 – S7; Table 2). The potentials were referenced against Fc/Fc^+ couple. The BODIPYs **1a – 1c** exhibit two oxidation and two reduction waves. The first oxidation corresponds to the ferrocenyl moiety, whereas the second oxidation and reduction waves correspond to the BODIPY moiety. The TCBD substituted BODIPYs **2a – 2c** exhibit two oxidation and four reduction waves. The additional two reduction waves correspond to the dianion formation of two dicyanovinyl moieties.

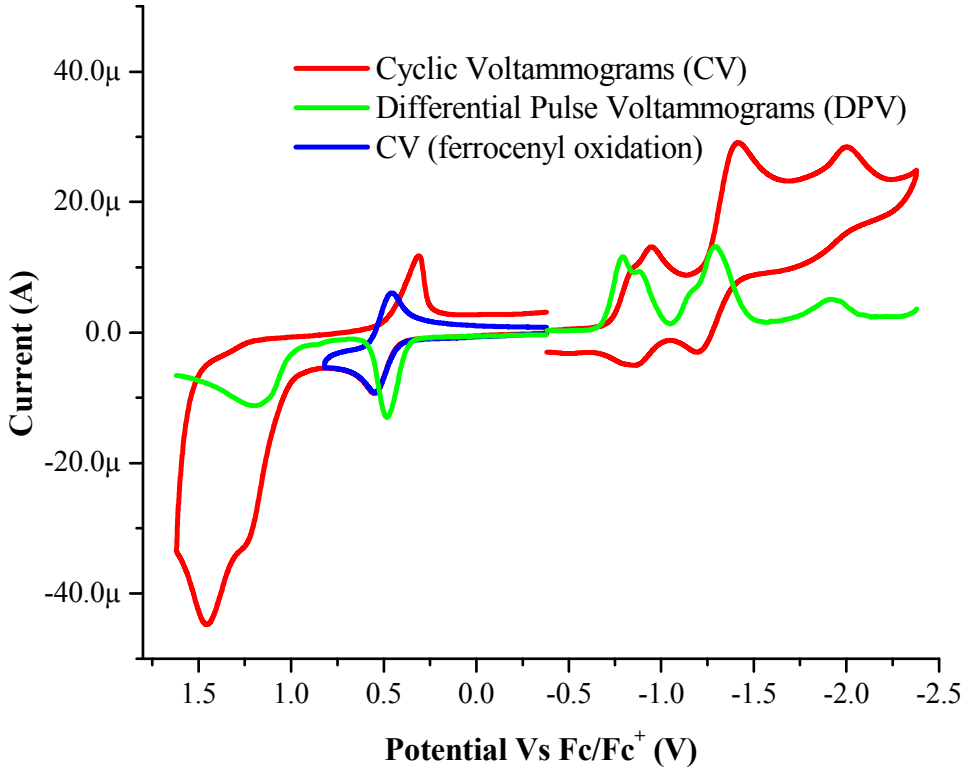

Figure 2. Overlaid Cyclic and differential pulse voltammograms (CV and DPV) of BODIPY **2b** recorded using glassy carbon as working electrode, Pt wire as the counter electrode, and saturated calomel electrode (SCE) as the reference electrode in CH_2Cl_2 solvent and 0.1 M tetrabutylammonium hexafluorophosphate as supporting electrolyte.

The first oxidation of BODIPYs **1a – 1c** follows the order **1a>1b>1c**. The first oxidation of BODIPY **1a** is much harder than the BODIPYs **1b** and **1c**, due to strong electronic coupling of ferrocene with electron deficient BODIPY in **1a**. The electron deficient BODIPY in **1a** withdraws the electron density from ferrocene making its oxidation harder. The introduction of TCBD in BODIPYs **2a – 2c** leads to two additional reduction waves and harder oxidation of ferrocene and BODIPY owing to electron deficient nature of TCBD. The distance between ferrocene and TCBD unit is constant in BODIPYs **2a – 2c**, hence the ferrocenyl oxidation reflects the electronic communication between the BODIPY and the TCBD unit. The ferrocenyl oxidation potential follows the order **2a>2b>2c**, indicating the strongly coupled TCBD and BODIPY units in **2a** followed by **2b** and **2c**. The strongly communicating TCBD and BODIPY

(in **2a**) becomes the stronger acceptor than weakly communicating TCBD and BODIPY (in **2c**). This is also reflected from the first reduction potential of **2a – 2c**. The BODIPY **2a** shows easier reduction than BODIPY **2b** and **2c** indicating the electron deficient nature of **2a**.[14]

The LUMOs of TCBD substituted BODIPYs are delocalized mainly on the TCBD, and slightly on BODIPY moiety (Figure 3), hence the reduction waves can be assigned to the reduction of TCBD moiety first, followed by the BODIPY moiety. This is also consistent with the literature reports as well.[13]

Table 2. The electrochemical properties of the ferrocenyl BODIPYs **1a – 1c** and **2a – 2c.**[a]

BODIPY	E^3 Oxid[b] (BODIPY)	E^2 Oxid[b] (BODIPY)	E^1 Oxid (Fc)	E^1 Red[b]	E^2 Red[b]	E^3 Red[b]	E^4 Red[b]
1a	-	1.03	0.25	-1.01	-1.28	-	-
2a	-	1.28	0.52	-0.35	-0.71	-1.32	-1.80
1b	-	1.12	0.11	-0.94	-1.34	-	-
2b	-	1.21	0.48	-0.79	-0.88	-1.16	-1.29
1c	-	1.17	0.10	-1.12	-1.41	-	-
2c	1.34	1.10	0.40	-0.73	-1.42	-2.03	-2.23

[a]The electrochemical analysis was performed in a 0.1 M solution of Bu_4NPF_6 in CH_2Cl_2 at 100 mVs^{-1} scan rate, versus Fc/Fc^+. [b]Irreversible or quasi reversible wave.

Computational Calculations

The computational calculations were performed using density functional theory (DFT)[15] at B3LYP/6-31G(d) level for C, N, B, F, H, and the Lanl2DZ level for Fe (the B3 exchange functional[16] and LYP correlation functional[17]). The DFT optimized geometries slightly differ from the X-ray structures. The comparison of optimized geometries with single crystal structures are displayed in Figure S5. The crystal structures and energy optimized structures slightly differ in bond length and bond angles, but differs significantly in the orientation of substituents. In the crystal structure of BODIPY **2c**, the biphenyl and BODIPY moiety are in *Z* configuration whereas in DFT optimized structures they are in *E* configuration. The torsional angles between the two dicyanovinyl moieties in the DFT optimized structure of **2a** and **2c** are 130.04° and 166.57°, whereas in the crystal structure the torsional angles are 55.79° and 75.41° respectively.

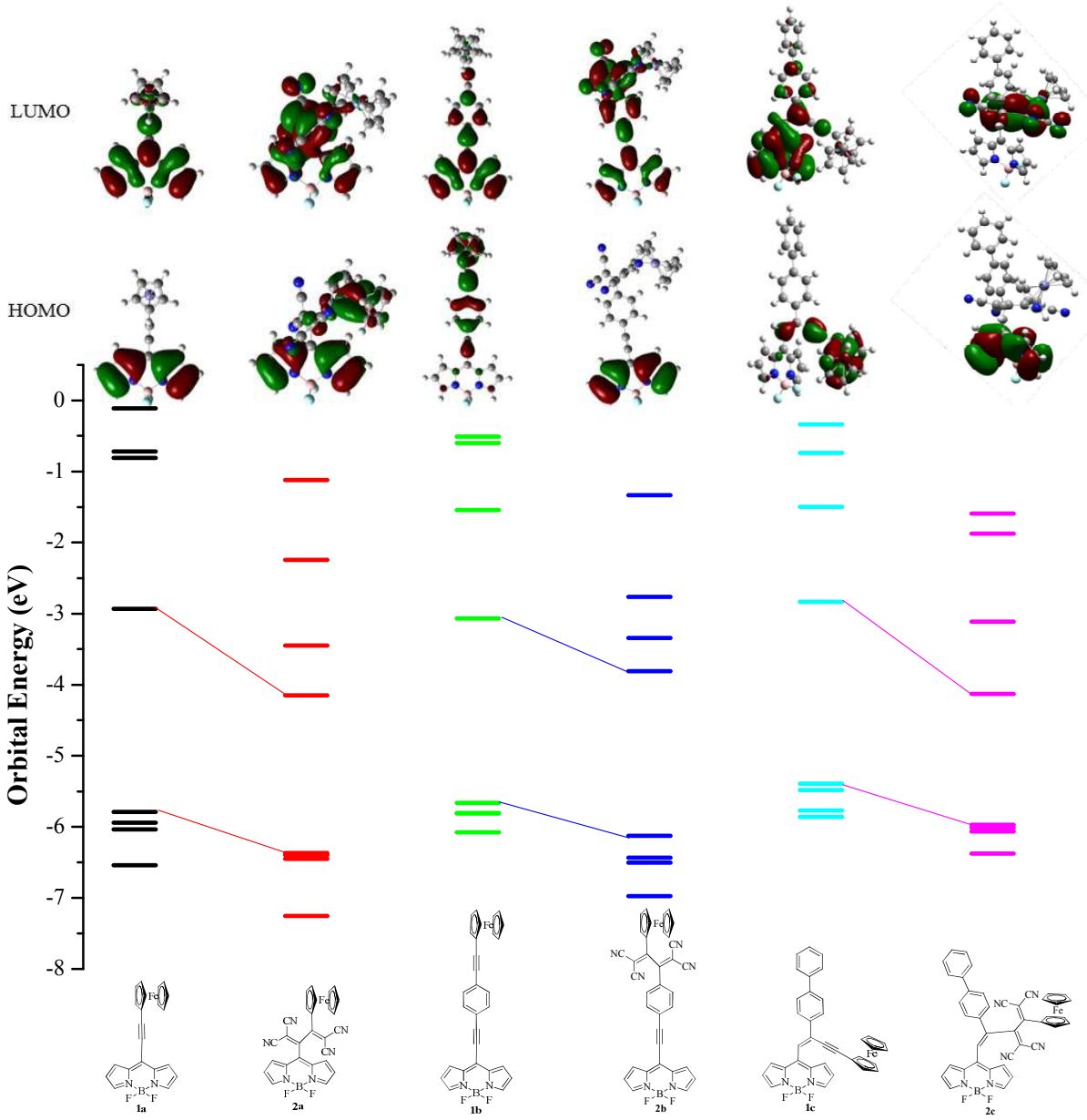

Figure 3. The comparison of frontier molecular orbitals and energy levels of BODIPYs **1a – 1c** and **2a – 2c**.

The frontier molecular orbital and electronic energy levels are displayed in Figure 3. In BODIPYs **1a – 1c** the LUMO is localized on the BODIPY unit, whereas the HOMO is localized on the BODIPY unit (in **1a**) and the ferrocenyl unit (in **1b** and **1c**), which suggests strong donor-acceptor (D-A) interaction between the donor ferrocene and acceptor BODIPY. The incorporation of TCBD stabilizes both the HOMO and LUMO orbitals. The node at the *meso* carbon in HOMO of BODIPYs **2a** and **2b** hinders the effective π-conjugation between *meso*

substituent and BODIPY in HOMO.[18] As a result the stabilization of HOMO is less pronounced than the LUMO, which leads to the lowering of HOMO-LUMO gap and red shift in the absorption. In case of BODIPY **2c** the LUMO is much stabilized and localized on the strong TCBD acceptor. The nature of the LUMO is entirely different in TCBD substituted BODIPYs and their precursors. In **1a – 1c** it is centered on the BODIPY whereas in **2a – 2c** on the newly generated TCBD acceptor and/or BODIPY unit. In BODIPYs **2a** and **2b** the LUMO is localized on the TCBD and BODIPY unit indicating strong electronic communication between the BODIPY and the TCBD unit. In BODIPY **2c** the LUMO is localized on the TCBD unit only, indicating weak electronic communication between the BODIPY and the TCBD.

The TD-DFT calculation was performed on TCBD substituted ferrocenyl BODIPYs **2a – 2c** to understand the origin of absorption bands. The TD-DFT calculation was performed by using B3LYP method at 6-31G(d) level in THF solvent using the IEFPCM formulation for solvent effects. The oscillator strengths and configurations of vertical transitions are shown in are included in the supporting information. In TD-DFT calculation of BODIPY **2a** the strongest band was observed at 437.08 nm corresponding to HOMO-2→LUMO+1 transition, followed by band at 345.79 nm corresponding to HOMO-2→LUMO+2 transition. In case of BODIPY **2b** the strongest band was observed at 457.42 nm and 457.78 nm corresponding to the HOMO-3→LUMO+1 and HOMO→LUMO+1 transition respectively. In case of BODIPY **2c** the strongest band was observed at 450.78 and 466.85 nm corresponding to the HOMO-3→LUMO+2, and HOMO-2→LUMO+2 respectively.

Crystal structure and packing

The single crystals of BODIPYs **2a** and **2c** were obtained by slow diffusion of hexane into the CH_2Cl_2 solution. The crystal structure and data refinement parameters are shown in Table S1 (ESI). The BODIPYs **2a** and **2c** crystallize into the monoclinic *P* 2_1/n space group. The TCBD unit disturbs the overall planarity of molecule but the BODIPY framework is planar with the boron atom slightly deviating from planarity (Figure 4). The crystal structures reveal extensive intermolecular hydrogen bonding interactions but no π-π stacking interaction due to loss of overall planarity.

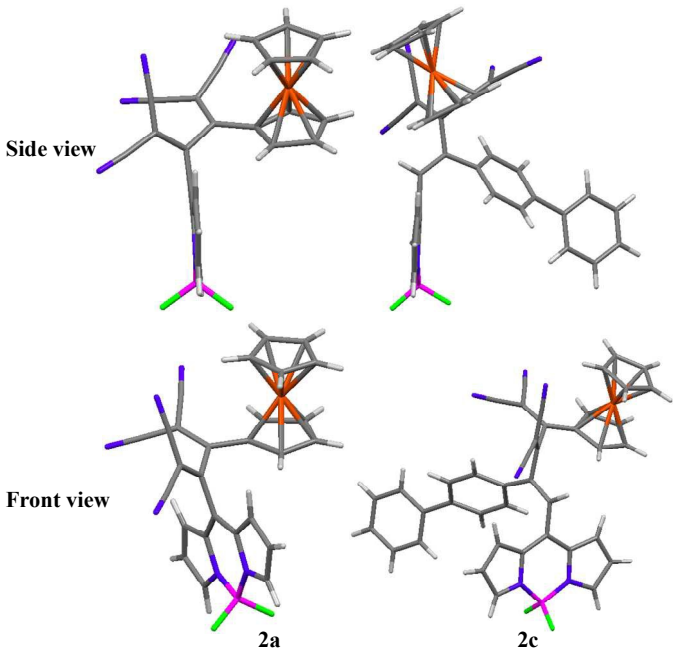

Figure 4. Side view and front view crystal structures of BODIPYs **2a** and **2c**.

In the crystal structure packing of BODIPY **2a**, two molecules connect to form dimeric framework through two mutual interaction C(1)-H(1)---F(1). These two dimers are connected to one another through another dimeric framework with interactions C(23)-H(23)---F(2) and C(7)-H(7)---F(2) leading to the 2D chain. These chains are further connected to each other via interaction C(25)-H(25)---N(6) to form complex 3D framework (Figure S3).

In the crystal structure packing of BODIPY **2c**, two mutual interactions between fluorine and *meso* vinyl proton and the ferrocenyl photon rigidifies a dimeric structure. The dimeric structures connect the one another diagonally via interactions C(29)-H(29)---F(1), C(37)-H(37)---N(4), C(41)-H(41)---π (Fc) and C(2)-H(2)---N(3) leading to two dimensional chain (Figure S4).

Conclusion

In summary, the reactivity of ferrocenyl BODIPYs towards the [2+2] cycloaddition-retroelectrocyclization reaction with tetracyanoethylene was studied, which follows the order **1b>1a>1c**. It was observed that the reactivity was influenced by; (i) The distance between the BODIPY unit and the alkyne unit, (ii) The electron donating/withdrawing substituents on the alkyne unit and (iii) Steric crowding. The TCBD substituted ferrocenyl BODIPYs exhibit strong D-A interactions. The ferrocenyl BODIPY where the alkyne unit and the BODIPY are well separated show high reactivity towards the [2+2] cycloaddition-retroelectrocyclization reaction

with tetracyanoethylene, whereas the ferrocenyl BODIPYs, where the alkyne unit is directly connected to the BODIPY show poor reactivity. The reactivity of ferrocenyl BODIPY **1c** was hindered due to the steric crowding. The electron withdrawing substituent at the *meso* position stabilizes both the HOMO and LUMO. The stabilization of HOMO was less pronounced compared to the stabilization of LUMO due to the presence of node at the *meso* carbon in HOMO. This leads to the red shifted absorption of TCBD substituted BODIPYs (**2a – 2c**) than their precursors (**1a – 1c**). The electrochemical properties reveal strong electronic communication between the BODIPY and the TCBD in **2a** followed by **2b** and **2c**. The results presented here will be helpful for the design of the smart materials with tunable properties for diverse applications.

Experimental Section

General methods. Chemicals were used as received unless otherwise indicated. All oxygen or moisture sensitive reactions were performed under nitrogen/argon atmosphere using standard Schlenk method. Triethylamine (TEA) was received from commercial source and distilled on KOH prior to use. ^{1}H NMR (400 MHz), and ^{13}C NMR (100MHz) spectra were recorded on the Bruker Avance (III) 400 by using $CDCl_3$ as solvent. ^{1}H NMR chemical shifts are reported in parts per million (ppm) relative to the solvent residual peak ($CDCl_3$, 7.26 ppm). Multiplicities are given as: s (singlet), d (doublet), t (triplet), q (quartet), dd (doublet of doublets), m (multiplet), and the coupling constants, *J*, are given in Hz. ^{13}C NMR chemical shifts are reported relative to the solvent residual peak ($CDCl_3$, 77.36 ppm). UV-visible absorption spectra of all compounds were recorded on a PerkinElmer's LAMBDA 35 UV/Vis Spectrophotometer. HRMS were recorded on Brucker-Daltonics, micrOTOF-Q II mass spectrometer. The voltammograms were recorded on a CHI620D electrochemical analyser in dichloromethane solvent and 0.1 M $TBAF_6$ as the supporting electrolyte. The electrodes used were glassy carbon as a working electrode, Pt

wire as a counter electrode and the saturated calomel electrode as a reference electrode. The potentials were referenced against Fc/Fc^+ as per IUPAC guidelines.

Synthetic procedure for the BODIPY 2a

Tetracyanoethylene (TCNE) (32 mg, 0.25 mmol) was added to a solution of compound **1a** (100 mg, 0.25 mmol) in CH_2Cl_2 (50 mL). The mixture was refluxed at 40 ºC for 8 hours. The solvent was removed in vacuum, and the product was purified by column chromatography with CH_2Cl_2 as the eluent to yield **2a** as a black green colored solid.

Black-green crystalline solid. Yield: 95 % (119 mg); ^{1}H NMR ($CDCl_3$, 400 MHz, ppm): δ 8.09 (s, 1H), 8.03 (s, 1H), 7.31-7.23 (m, 2H), 6.79 (m, 1H), 6.70 (m 1H), 5.37 (s, 1H), 5.09 (s, 1H), 4.96 (s, 1H), 4.88 (s, 1H), 4.41 (s, 5H); ^{11}B NMR ($CDCl_3$, 128 MHz, ppm) 0.09 (t, J_{B-F} = 28.1 Hz); UV/vis (TOLUENE): λ_{max} (ε [$M^{-1}cm^{-1}$]) 567 (2.22× 10^4). HRMS (ESI-TOF) m/z = calculated for $C_{27}H_{15}BF_2FeN_6$ = 551.0670 $[M+Na]^+$, measured 551.0666 $[M+Na]^+$.

Synthetic procedure for the BODIPY 2b

Tetracyanoethylene (TCNE) (26 mg, 0.20 mmol) was added to a solution of compound **1b** (100 mg, 0.20 mmol) in CH_2Cl_2 (50 mL). The mixture was stirred at room temperature for 2 hours. The solvent was removed in vacuum, and the product was purified by column chromatography with CH_2Cl_2 as the eluent to yield **2b** as a dark purple colored solid.

Dark purple crystalline solid. Yield: 95 % (119 mg); ^{1}H NMR ($CDCl_3$, 400 MHz, ppm): δ 7.86 (s, 2H), 7.78-7.75 (m, 2H), 7.68-7.66 (m, 2H), 7.34-7.33 (d, 2H, J = 4Hz), 6.57-6.56 (d, 2H, J = 4Hz), 5.46-5.45 (m, 1H), 5.07-5.05 (m, 1H), 4.90-4.89 (m, 1H), 4.52-4.51 (m, 1H), 4.46 (s, 5H). ^{13}C NMR ($CDCl_3$, 100 MHz, ppm): 171.7, 164.9, 144.8, 136.6, 133.5, 132.7, 129.4, 128.9, 126.6, 125.3, 119.0, 113.5, 113.0, 111.4, 111.3, 101.4, 87.6, 87.3, 78.7, 76.3, 75.3, 74.5, 72.9, 71.3; ^{11}B NMR ($CDCl_3$, 128 MHz, ppm) 0.14 (t, J_{B-F} = 28.16 Hz); UV/vis (TOLUENE): λ_{max} (ε [$M^{-1}cm^{-1}$])

561 (2.31× 10^4). HRMS (ESI-TOF) m/z = calculated for $C_{35}H_{19}BF_2FeN_6$ = 651.0981 $[M+Na]^+$, measured 651.0964 $[M+Na]^+$.

Synthetic procedure for the BODIPY 2c

Tetracyanoethylene (TCNE) (22 mg, 0.17 mmol) was added to a solution of compound **1c** (100 mg, 0.17 mmol) in CH_2Cl_2 (50 mL). The mixture was refluxed at 40 ºC for 7 days. The solvent was removed in vacuum, and the product was purified by column chromatography with CH_2Cl_2 as the eluent to yield **2c** as a black-green colored solid.

Black-green crystalline solid. Yield: 95 % (110 mg); ^{1}H NMR ($CDCl_3$, 400 MHz, ppm): δ 7.77 (s, 2H), 7.49-7.46 (m, 2H), 7.45-7.35 (m, 5H), 7.34 (s, 1H), 7.08-7.05 (m, 2H), 6.97 (d, 2H, J = 4.28), 6.45-6.43 (m, 2H), 5.41-5.40 (m, 1H), 5.08-5.06 (m, 1H), 5.03-5.01 (m, 1H), 4.67-4.66 (m, 1H), 4.50 (s, 5H); ^{13}C NMR ($CDCl_3$, 100 MHz, ppm): 176.0, 167.4, 145.8, 143.9, 143.7, 134.2, 133.5, 130.8, 130.1, 130.0, 129.2, 128.5, 128.1, 127.4, 127.2, 123.4, 122.1, 119.6, 100.4, 76.5, 75.3, 74.9, 73.9, 73.4, 70.8; ^{11}B NMR ($CDCl_3$, 128 MHz, ppm) -0.09 (t, J_{B-F} = 28.16 Hz); UV/vis (TOLUENE): λ_{max} (ε [$M^{-1}cm^{-1}$]) 521 (1.84 × 10^4). HRMS (ESI-TOF) m/z = calculated for $C_{41}H_{25}BF_2FeN_6$ = 729.1451 $[M+Na]^+$, measured 729.1480 $[M+Na]^+$.

Associated Content

Supporting Information

† Text, figures, tables, and CIF files giving general experimental methods, ^{1}H, ^{13}C, and ^{11}B NMR and HRMS spectra of all new compounds, crystallographic data for **2a** and **2b** (CCDC numbers 1414197 and 1414196 respectively), DFT calculation data and electrochemical studies. This material is available free of charge via the internet at DOI: 10.1039/b000000x/

Author Information

Corresponding Author

* *Fax: +91 731 2361 482, E-mail: rajneeshmisra@iiti.ac.in*

Acknowledgement

We thank DST, New Delhi for financial support. BD and TJ thank CSIR and UGC New Delhi for their fellowships. We are thankful to Sophisticated Instrumentation Centre (SIC), IIT Indore.

References

1 (a) H. L. Dong, H. F. Zhu, Q. Meng, X. Gong, W. P. Hu, *Chem. Soc. Rev.,* 2012, **41**, 1754–1808; (b) Y. Li, T. Liu, Liu, H. Liu, M. Z. Tian, Y. Li, *Acc. Chem. Res.,* 2014, **47**, 1186; (c) M. Gjhyilbert, B. Albinsson, *Chem. Soc. Rev.,* 2015, **44**, 845–862; (d) R. Gompper, H.-U. Wagner, *Angew. Chem., Int. Ed.*, 1988, **27**, 1437–1455; (e) M. Kivala, C. Boudon, J.-P. Gisselbrecht, P. Seiler, M. Gross, F. Diederich, *Angew. Chem., Int. Ed.,* 2007, **46**, 6357– 6360; (f) J. C. May, I. Biaggio, F. Bures, F. Diederich, *Appl. Phys. Lett.,* 2007, **90**, 251106.

2 (a) H. Lu, J. Mack, Y. Yang, Z. Shen, *Chem. Soc. Rev.,* 2014, **43**, 4778; (b) A. Loudet, K. Burgess, *Chem. Rev.,* 2007, **107**, 4891; (c) J. Han, K. Burgess, *Chem. Rev.,* 2010, **110**, 2709.

3 Long, N. J. *Angew. Chem.,* 1995, **107**, 37– 56; *Angew. Chem., Int. Ed.,* 1995, **34**, 21– 38.

4 (a) B. Dhokale, P. Gautam, S. M. Mobin, R. Misra, *Dalton Trans.*, 2013, **42**, 1512; (b) R. Misra, B. Dhokale, T. Jadhav, S. M. Mobin, *Organometallics*, 2014, **33**, 1867–1877; (c) R. Misra, B. Dhokale, T. Jadhav, S. M. Mobin, *Dalton Trans.,* 2014, **43**, 4854; (d) R. Misra, B. Dhokale, T. Jadhav, S. M. Mobin, *New J. Chem.,* 2014, **38**, 3579; (d) R. Misra, T. Jadhav, B. Dhokale, P. Gautam, R. Sharma, R. Maragani, S. M. Mobin, *Dalton Trans.,* 2014, **43**, 13076; (e) J. O. Flores-Rizo, I. Esnal, C. A. Osorio-Martínez, C. F. A. Gómez-Durán, J. Bañuelos, I. López Arbeloa, K. H. Pannell, A. J. Metta-Magaña, E. Peña-Cabrera, *J. Org. Chem.*, 2013, **78**, 5867; (f) X. Yin, Y. Li, Y. Li, Y. Zhu, X. Tang, H. Zheng and D. Zhu, *Tetrahedron*, 2009, **65**, 8373–8377; (g) X. Yin, Y. Li, Y. Zhu, X. Jing, Y. Li and D. Zhu, *Dalton Trans.*, 2010, **39**, 9929–9935; (h) P. Gautam, B. Dhokale, V. Shukla, C. P. Singh, K. S. Bindra and R. Misra, *J. Photochem. Photobiol., A*, 2012, **239**, 24–27; (i) T. Jadhav, R. Maragani, R. Misra, V. Sreeramulu, D. N. Rao and S. M. Mobin,*Dalton Trans.*, 2013, **42**, 4340–4342.

5 B. Dhokale, T. Jadhav, S. M. Mobin, R. Misra, *Dalton Trans.*, 2015, DOI: 10.1039/C5DT00565E.

6 (a) T. Shoji, A. Maruyama, C. Yaku, N. Kamata, S. Ito, T. Okujima, K. Toyota, *Chem. Eur. J.,* 2015, **21**, 402–409; (b) T. Shoji, S. Ito, K. Toyota, M. Yasunami, N. Morita, *Chem.–Eur. J.*, 2008, **14**, 8398–8408; (c) C. Dengiz, B. Breiten, J.-P. Gisselbrecht, C. Boudon, N. Trapp, W. B. Schweizer,

F. Diederich, *J. Org. Chem.,* 2015, **80**, 882−896; (d) S.-i. Kato, M. Kivala, W. B. Schweizer, C. Boudon, J.-P. Gisselbrecht, F. Diederich, *Chem. Eur. J.,* 2009, **15**, 8687–8691.

7 B. Dhokale, T. Jadhav, S. M. Mobin, R. Misra, *RSC Adv*., 2015, **5**, 57692-57699.

8 (a) R. Misra, B. Dhokale, T. Jadhav, S. M. Mobin, *Dalton Trans.,* 2014, **43**, 4854; (b) R. Misra, B. Dhokale, T. Jadhav, S. M. Mobin, *New J. Chem.,* 2014, **38**, 3579; (c) R. Misra, T. Jadhav, B. Dhokale, P. Gautam, R. Sharma, R. Maragani, S. M. Mobin, *Dalton Trans.,* 2014, **43**, 13076; (d) J. O. Flores-Rizo, I. Esnal, C. A. Osorio-Martínez, C. F. A. Gómez-Durán, J. Bañuelos, I. López Arbeloa, K. H. Pannell, A. J. Metta-Magaña, E. Peña-Cabrera, *J. Org. Chem.*, 2013, **78**, 5867; (e) B. Dhokale, T. Jadhav, S. M. Mobin, R. Misra, *J. Org. Chem.,* 2015, **80**, 8018–8025.

9 R. Misra, B. Dhokale, T. Jadhav, S. M. Mobin, *Dalton Trans.,* 2013, **42**, 13658.

10 B. Dhokale, T. Jadhav, S. M. Mobin, R. Misra, *Dalton Trans.*, 2015, DOI: 10.1039/C5DT00565E.

11 (a) A. D. Finke, O. Dumele, M. Zalibera, D. Confortin, P. Cias, G. Jayamurugan, J.-P. Gisselbrecht, C. Boudon, W. B. Schweizer, G. Gescheidt, F. Diederich, *J. Am. Chem. Soc.,* 2012, **134**, 18139; (b) M. Jordan, M. Kivala, C. Boudon, J.-P. Gisselbrecht, W. B. Schweizer, P. Seiler, F. Diederich, *Chem.—Asian J.,* 2011, **6**, 396– 401.

12 N. Kraußе, M. Kielmann, J. Ma, H. Butenschön, *Eur. J. Org. Chem.,* 2015, 2622– 2631.

13 (a) Niu, S.; Ulrich, G.; Retailleau, P.; Ziessel, R. *Org. Lett.,* 2011, **13**, 4996– 4999; (b) Niu, S.; Ulrich, G.; Retailleau, P.; Ziessel, R. *Tetrahedron Lett.,* 2011, **52**, 4848– 4853.

14 (a) S.-i. Kato, F. Diederich, *Chem. Commun.,* 2010, **46**, 1994– 2006; (b) P. Retenauer, M. Kivala, P. D. Jarowski, C. Boudon, J.-P. Gisselbrecht, M. Gross, F. Diederich, *Chem. Commun.,* 2007, 4898.

15 M. J. Frisch, G. W. Trucks, H. B. Schlegel, G. E. Scuseria, M. A. Robb, J. R. Cheeseman, G. Scalmani, V. Barone, B. Mennucci, G. A. Petersson, H. Nakatsuji, M. Caricato, X. Li, H. P. Hratchian, A. F. Izmaylov, J. Bloino, G. Zheng, J. L. Sonnenberg, M. Hada, M. Ehara, K. Toyota, R. Fukuda, J. Hasegawa, M. Ishida, T. Nakajima, Y. Honda, O. Kitao, H. Nakai, T. Vreven, J. J. A. Montgomery, J. E. Peralta, F. Ogliaro, M. Bearpark, J. J. Heyd, E. Brothers, K. N. Kudin, V. N. Staroverov, R. Kobayashi, J. Normand, K. Raghavachari, A. Rendell, J. C. Burant, S. S. Iyengar, J. Tomasi, M. Cossi, N. Rega, J. M. Millam, M. Klene, J. E. Knox, J. B. Cross, V. Bakken, C. Adamo, J. Jaramillo, R. Gomperts, R. E. Stratmann, O. Yazyev, A. J. Austin, R. Cammi, C. Pomelli, J. W. Ochterski, R. L. Martin, K. Morokuma, V. G. Zakrzewski, G. A. Voth, P. Salvador,

J. J. Dannenberg, S. Dapprich, A. D. Daniels, O. Farkas, J. B. Foresman, J. V. Ortiz, J. Cioslowski and D. J. Fox, *Gaussian09, Revisions, A.02*, Gaussian, Inc., Wallingford, CT, 2009.

16 A. D. Becke, *J. Chem. Phys*., 1993, **98**, 5648–5652.

17 C. Lee, W. Yang and R. G. Parr, Phys. Rev. B: Condens. *Matter Mater. Phys*., 1988, **37**, 785.

18 (a) S. Kusaka, R. Sakamoto, Y. Kitagawa, M. Okumura, H. Nishihara, *Chem. – Asian J.,* 2013, **8**, 723;
(b) K. Graf, T. Korzdorfer, S. Kummel, M. Thelakkat, *New J. Chem.,* 2013, **37**, 1417.